Extended three-body-force shell model dynamics of heavier alkali-halide crystals

R. K. Singh, H. N. Gupta, and M. K. Agrawal
Solid State Research Centre, Department of Physics, N.R.E.C. College, Meerut University, Khurja-203131, India
(Received 26 April 1976; revised manuscript received 24 November 1976)

The lattice dynamics of heavier alkali halides have been thoroughly investigated by means of an extended three-body-force shell model (ETSM) developed by Singh and his collaborators. The theoretical predictions achieved for the phonon dispersions, two-phonon Raman scattering and infrared-absorption spectra, and Debye-temperature variations in the rubidium and cesium halides are in reasonably good agreement with the experimental data. On the basis of such overall fair agreement, the ETSM can be regarded as an adequate and appropriate model for the dynamical description of alkali halides. It is also interesting to note that ETSM is capable of describing the dynamical and dielectric properties of heavier alkali halides with the same success as it does for the light-weight alkali halides.

I. INTRODUCTION

Recently, Singh and co-workers[1-4] have developed an extended three-body-force shell model (ETSM) for the lattice dynamics of ionic solids. Its development is based on the incorporation of the effects of long-range three-body forces[5-7] and the extension of short-range two-body overlap repulsion from first- to second-neighbor ions in the conventional framework of both ions polarizable rigid-shell model[8] (RSM). The framework of ETSM is essentially an amalgamation of two most commonly used and realistic phenomenological models, namely, the RSM and deformation-dipole model[9] (DDM). This is evident from the fact that ETSM contains (a) the two-body long-range Coulomb interactions and short-range overlap repulsion operative up to the second-neighbor ions, (b) the long-range three-body forces arising from the deformation of the electron shells, and (c) the dipole character of the constituent ions owing its origin to the relative displacement between cores and shells.

The framework of ETSM has some additional features as compared to the original TSM[7,10-14] (OTSM). This can be noted from the facts that (i) the off-diagonal elements of the dynamical matrix contains a completely new and significant term besides minor modifications introduced in various other quantities involved in them; (ii) the ETSM framework is free from inconsistencies present in OTSM due to inadvertant error in the definition of ionic, core, and shell charges; (iii) the three-body forces introduce important modifications in various macroscopic relations namely the Lorentz-Lorenz, Clausius-Mosotti, Ruffa, and Szigeti relations and leave the well-known Lyddane-Sachs-Teller relations unchanged.

Until now the ETSM has been applied successfully to describe the lattice dynamics of thallous bromide,[1] sodium halides,[2] and cesium fluoride.[3] However, on the basis of this success alone the versatility of ETSM cannot be generalized without carrying out thorough investigation for the remaining members of this family. The necessity for such an investigation is also pertinent in view of the Hardy's remark[15,16] that no one model is equally good for all the alkali halides, i.e., if a given model in its simplest form is good for sodium (or lithium) halides the same model may be much less satisfactory for rubidium (or cesium) halides. In the first two cases the positive ions are light and of low polarizability, whereas for the second two cases the reverse is true.

This basic need motivated the present authors to study the lattice dynamics of heavier alkali halides employing ETSM. The choice of these solids as subjects of investigation has several other motives also. Firstly, they are characterized by large Cauchy violations, high dielectric constants, and extremely large electronic polarizabilities and ionic radii of the cations. Secondly, the OTSM[10-13] being subject to some limitations[1,2] has given a poor description of the lattice dynamics of rubidium[13] and cesium[14] halides. The reason for poor description in case of cesium halides[14] may be ascribed to the error inherent in the model formalism. The three-body contributions to C_{11} and C_{12} are erroneous by a factor $\sqrt{3}$ in view of the fact that these authors[14] have written $(a\,df/dr)_0$ instead of $3^{-1/2}r_0(df/dr)_0$ with $2a$ and r_0 as lattice constant and nearest-neighbor separation, respectively. Also, the contribution of second-neighbor interactions to C_{11} estimated by them[14] is twice as large as it should be. Furthermore, the overlap parameters of Lal and Verma[14] carry a factor of 2 which is inconsistent with the equilibrium condition [their[14] equation (2)].

The present work includes the predictions of the phonon-dispersion relations, two-phonon Raman

TABLE I. Input data for model calculation. f is superscript used to designate free-ion state.

Properties		RbF Value	RbF Ref.	RbCl Value	RbCl Ref.	RbBr Value	RbBr Ref.	RbI Value	RbI Ref.
Elastic constants	C_{11}	5.100	17	4.298	22	3.863	24	3.210	24
(10^{11} dyn cm^{-2})	C_{12}	1.370	17	0.676	22	0.474	24	0.360	24
	C_{44}	0.980	17	0.492	22	0.405	24	0.292	24
Polarizability ratio	$(\alpha_1/\alpha_2)^f$	1.346	18	0.382	18	0.475	25	0.307	25
Vibration frequencies	$\omega_{TO}(\Gamma)$	3.055	17	2.360	17	1.760	26	1.530	27
(10^{13} rad sec^{-1})	$\omega_{LO}(L)$	4.700	17	2.750	17	1.820[a]	26	1.680	27
	$\omega_{LA}(L)$	2.380	17	1.910	17	1.760	26	1.224[a]	27
	$\omega_{TO}(L)$	3.140	17	2.150	17	1.315[a]	26	1.210	27
	$\omega_{TA}(L)$	1.386	17	1.320	17	1.315	26	1.050[a]	27
Dielectric constants	ϵ_0	5.910	19	3.990	b	4.510	20	4.200	b
	ϵ_α	1.940	20	2.200	20	2.250	b	2.610	20
Interionic distance (10^{-8} cm)	r_0	2.7985	21	3.245	23	3.399	23	3.6275	23

[a] Extrapolated values.

[b] Calculated from Lyddane-Sachs-Teller relation using $\omega_{LO}(\Gamma)$ equal to 3.18, 2.49, and 1.94 for RbCl (Ref. 17), RbBr (Ref. 26), and RbI (Ref. 27), respectively.

scattering and infrared absorption spectra, and Debye-temperatures variations in rubidium and cesium halides. In general, theoretical predictions and experimental observations are in reasonably good agreement. A detailed discussion of the results revealed by ETSM will be presented a little later.

II. RESULTS AND DISCUSSION

The ETSM theory described elsewhere[1,2] contains 12 parameters out of which there are six parameters for the overlap repulsion ($A_{12}, B_{12}, A_{11}, B_{11}, A_{22}, B_{22}$), two for three-body interactions ($f_0, r_0 f_0'$) and four for electrical and mechanical polarizabilities ($\alpha_1, \alpha_2, d_1, d_2$). Here, the subscripts 1 and 2 refer to cations and anions, respectively. The strategy for their determination is exactly the same as followed earlier.[1,2] The macroscopic data used are three elastic constants, five vibration frequencies, two dielectric constants, lattice constant, and ratio of free-ion electrical polarizabilities. The input data used are listed in Tables I and II while the values of model parameters are given in Tables III and IV. The calculations performed with the knowledge of these parameters are discussed in the following.

A. Phonon spectra

The phonon spectra for the present system of solids have been calculated for a mesh of 1000

TABLE II. Input data for model calculations.

Property		CsCl (78 °K) Values	CsCl (78 °K) Ref.	CsCl (RT)[a] Values	CsCl (RT)[a] Ref.	CsBr (80 °K) Values	CsBr (80 °K) Ref.	CsI (RT)[a] Values	CsI (RT)[a] Ref.
Elastic constant	C_{11}	4.260	28	4.068	30	3.349	31	2.434	31
(10^{11} dyn/cm^2)	C_{12}	1.300	28	1.200	30	1.002	31	0.636	31
	C_{44}	1.092	28	1.100	30	0.962	31	0.666	31
Vibration frequencies	$\nu_{TO}(\Gamma)$	3.170	20	3.030	29	2.355	32	1.961	34
(10^{12} sec^{-1})	$\nu_{LO}(R)$	3.850	29	3.760	29	2.404	32	1.815	34
	$\nu_{LA}(R)$	2.020	29	1.970	29	1.894	32	1.719	34
	$\nu_{TO}(X)$	2.980	29	2.850	29	1.910	32	1.214	34
	$\nu_{TA}(X)$	1.310	29	1.270	29	1.320	32	1.266	34
Polarizability ratio	$(\alpha_1/\alpha_2)^f$	1.055	25	1.055	25	0.759	25	0.506	20
Dielectric constant	ϵ_0	6.680	20	6.950	20	6.390	20	6.540	20
	ϵ_α	2.670	20	2.630	20	2.830	20	3.020	20
Lattice constant (Å)	$2a$	4.088	29	4.123	29	4.286	33	4.567	33

[a] RT, room temperature.

TABLE III. Model parameters of rubidium halides.

ETSM				Model parameters	TSM			
RbI	RbBr	RbCl	RbF		RbF	RbCl	RbBr	RbI
12.500	12.304	11.455	10.274	A_{12}	10.195	11.800	12.226	12.655
−0.637	−0.715	−0.724	−0.874	B_{12}	−0.873	−0.792	−0.785	−0.734
0.331	−0.475	−0.175	0.525	A_{11}	...	...	...	...
−0.116	0.184	0.036	−0.175	B_{11}	...	...	...	...
−0.175	0.400	0.107	−0.524	A_{22}	...	...	...	...
0.272	−0.255	−0.105	0.176	B_{22}	...	...	...	...
−0.031	−0.027	−0.027	−0.021	f_0	−0.021	−0.027	−0.027	−0.031
0.022	0.017	0.038	0.045	$r_0 f_0'$	0.045	0.038	0.017	0.022
−19.722	−15.294	−15.276	−11.260	Y_1	−10.849	−56.475	−9.725	−28.702
−4.234	−10.012	−2.637	−7.479	Y_2	−2.455	−1.856	−3.147	−2.703
0.010	0.015	0.011	0.021	d_1	0.025	0.004	0.028	0.008
0.155	0.048	0.162	0.023	d_2	0.082	0.295	0.180	0.279

wave-vector points in the first Brillouin zone. This division due to symmetry properties of Brillouin zone corresponds to 48 and 56 nonequivalent points for sodium- and cesium-chloride structures, respectively. The phonon-dispersion curves are displayed in Figs. 1–8 along principal symmetry directions together with neutron-scattering data on them.

A close inspection of Figs. 1–4 clearly demonstrates that the general agreement between theoretical and experimental phonon-dispersion curves for rubidium halides obtained by ETSM is faily good, while the same achieved with pre-[35,36] and post-[13,37–40] experimental models is not so good. The agreement obtained by Karo[35] with DDM[9] is extremely poor as compared to the present results. This disagreement is not unexpected because DDM takes account of only the electron-shell deformations while their overlap and displacement effects are significant in solids like rubidium halides which possess considerable Cauchy discrepancies and large positive-ion polarizabilities and ionic radii. Efforts by Karo[36] to improve the DDM by introducing next-nearest-neighbor effects have provided the interpretation of RbF and RbCl but with only moderate success.

The agreement reported by Sneh and Dayal,[37] Pandey and Dayal,[38] and Kress[39] are also only moderately satisfactory. The first two authors have used RSM[8] while the last one has used breathing-shell model.[41] The degree of agreement obtained by Lal and Verma[13] with OTSM[7,10] is comparable with ETSM but its framework suffers from several drawbacks as pointed out earlier. The experimental investigators have generally employed different versions of RSM to interpret their results on the phonon dispersion for the present system of solids. These models yield exact agreement, comparable with those obtained by ETSM, but some of their parameters attain unphysical

TABLE IV. Model parameters.

Parameters	Values			
	CsCl (78 °K)	CsCl (RT)[a]	CsBr (80 °K)	CsI (RT)
f_0	−0.009 25	−0.008 86	−0.008 92	0.006 41
$r_0 f_0'$	0.011 60	0.005 77	0.002 71	−0.002 63
A_{12}	4.381 37	4.259 10	4.589 70	5.265 80
B_{12}	−0.260 86	−0.233 81	−0.169 23	−0.289 66
A_{11}	0.170 83	0.093 50	0.013 51	−0.587 31
B_{11}	−0.049 74	−0.020 89	−0.092 33	+0.053 00
A_{22}	0.088 56	0.226 95	0.127 14	0.000 50
B_{22}	−0.006 72	−0.092 51	−0.012 53	−0.121 94
d_1	0.040 08	0.044 62	0.072 87	0.014 53
d_2	0.129 45	0.119 23	0.157 71	0.238 73
Y_1	−10.518 91	−9.450 40	−5.977 40	−28.084 00
Y_2	−3.087 34	−3.352 70	−3.636 30	−3.377 50

[a] RT, room temperature.

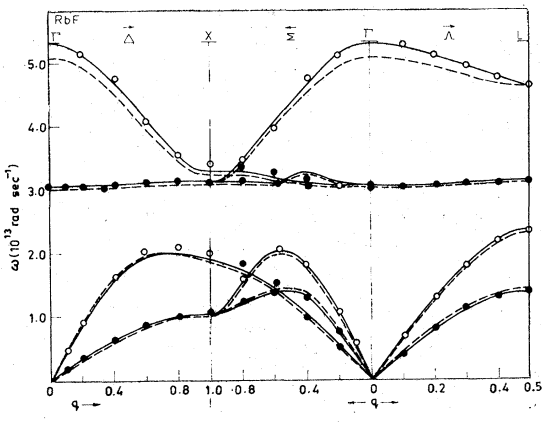

FIG. 1. Phonon-dispersion curves for RbF. Theoretical curves: solid line, ETSM; dashed line, TSM. Experimental points (Ref. 17): ○, longitudinal; ●, transverse.

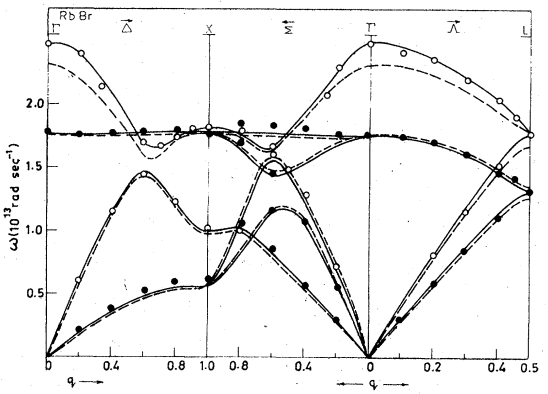

FIG. 3. Phonon-dispersion curves for RbBr. Theoretical curves: solid line, ETSM; dashed line, TSM. Experimental points (Ref. 26): ○, longitudinal; ●, transverse.

values.

The importance of second-neighbor interactions has been visualized in Figs. 1–4 where the phonon-dispersion curves obtained with and without their effects have been plotted. The role of second-neighbor interactions is quite obvious from the relative agreement achieved with TSM and ETSM. The contributions of these forces have increased consistently and reasonably from RbF to RbI. Also, their effects are more prominent in optical branches than in acoustic ones with few exceptions. The ETSM has predicted a large energy gap between the optical and acoustic branches in the case of solids in which the mass of the ions differ appreciably (RbF and RbCl) and the absence of such a gap in the case of solids with comparable ionic masses (RbBr and RbI). This feature is in accordance with the observations of Rolandson.[42]

A look at the Figs. 5–8 shows that the phonon-dispersion curves derived from ETSM are in quite good agreement with those measured by the neutron-spectroscopic technique for cesium halides. The dispersion curves derived from the pre-experimental models, namely, the rigid-ion model,[43-46] modified rigid-ion model,[47] RSM,[33,40,48,49] DDM,[50] and breathing-shell model,[30,31,51] do not agree so well with the measured ones. The efforts devoted after the report of accurately measured neutron-scattering data on CsCl,[29] CsBr,[32,52] and CsI,[34] have employed more elaborate models (RSM and breathing-shell model) to predict them but with only moderate success. It is interesting to note from the Figs. 6 and 8 that the harmonic ETSM has predicted the phonon-dispersion curves

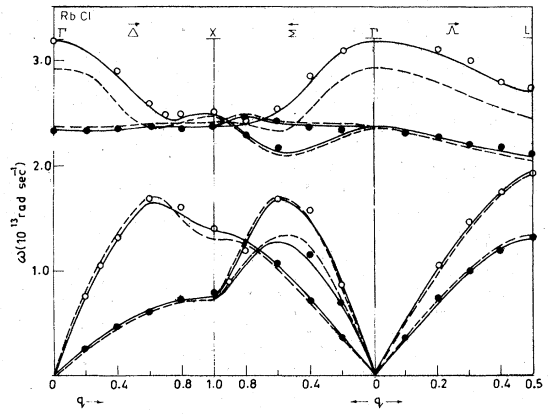

FIG. 2. Phonon-dispersion curves for RbCl. Theoretical curves: solid lines, ETSM; dashed line, TSM. Experimental points (Ref. 17): ○, longitudinal; ●, transverse.

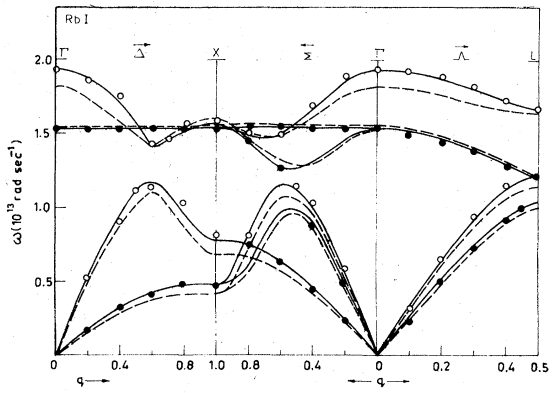

FIG. 4. Phonon-dispersion curves for RbI. Theoretical curves: solid line, ETSM; dashed line, TSM. Experimental points (Ref. 27): ○, longitudinal; ●, transverse.

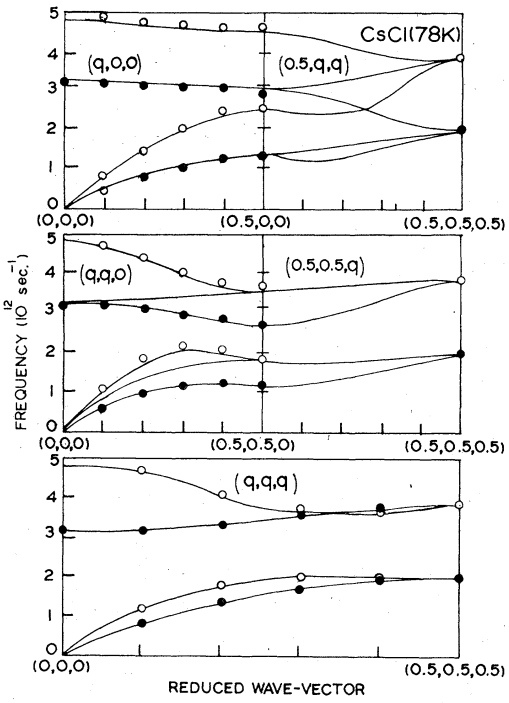

FIG. 5. Dispersion curves for CsCl at 78 K. Theoretical curves (ETSM). Experimental points (Ref. 29) (○, longitudinal; ●, transverse).

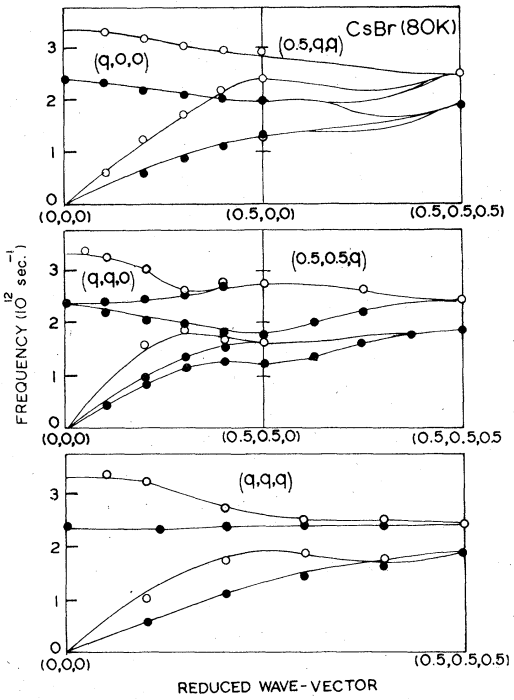

FIG. 7. Dispersion curves for CsBr at 80 K. Theoretical curves (ETSM). Experimental points (Ref. 32) (○, longitudinal; ●, transverse).

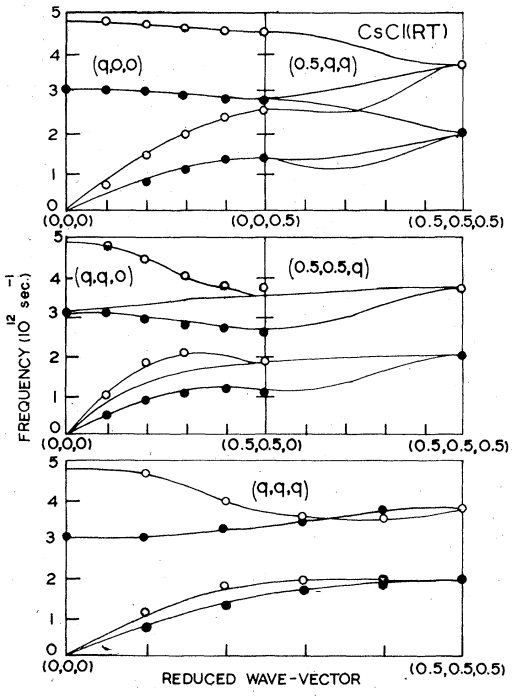

FIG. 6. Dispersion curves for CsCl at 298 K. Theoretical curves (ETSM). Experimental points (Ref. 29) (○, longitudinal; ●, transverse).

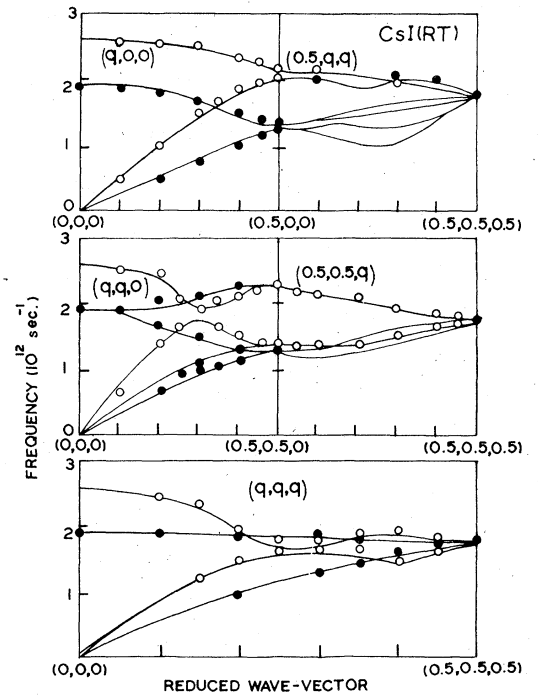

FIG. 8. Dispersion curves for CsI at 300 K. Theoretical curves (ETSM). Experimental points (Ref. 34) (○, longitudinal; ●, transverse).

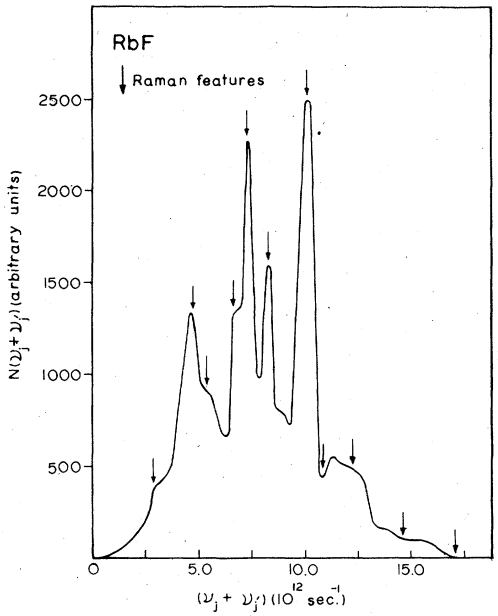

FIG. 9. Combined-density-of-states curve for RbF. The arrows indicate the measured peaks (Ref. 54).

at 298 K for CsCl and CsI equally well as for CsCl and CsBr at 80 K (see Figs. 5 and 7).

Since some of the vibration frequencies of zone-boundary points have been used to determine the model parameters, therefore, good agreement achieved for symmetry directions does not essentially guarantee the agreement in the other general directions. Thus, the validity of the model has been tested for off-symmetry directions by deriving the physical properties associated with complete phonon spectra.

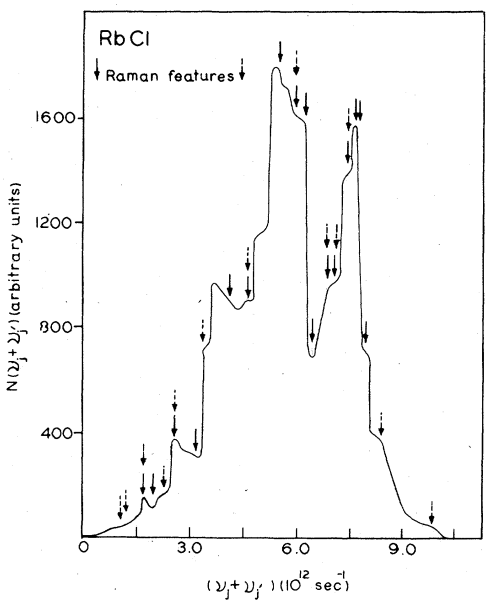

FIG. 10. Combined-density-of-states curve for RbCl. The solid and broken arrows indicate the measured peaks corresponding to Ref. 55 and 56, respectively.

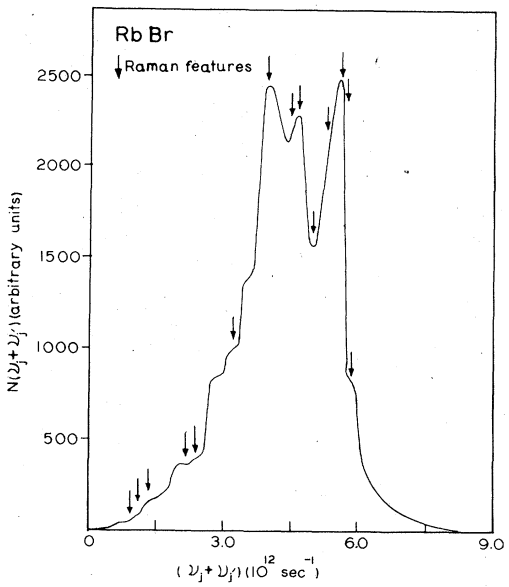

FIG. 11. Combined-density-of-states curve for RbBr. The arrows indicate the measured peaks (Ref. 55).

B. Derivable physical properties

The physical properties derivable easily from the phonon spectra are the second-order Raman

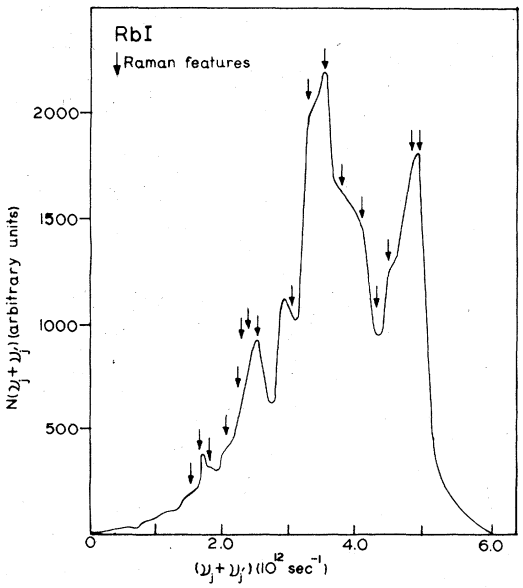

FIG. 12. Combined-density-of-states curve for RbI. The arrows indicate the measured peaks (Ref. 55).

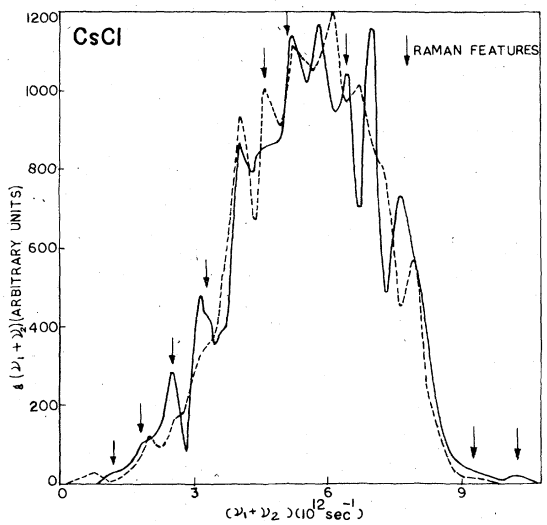

FIG. 13. Combined-density-of-states curves for CsCl. Solid and dashed curves correspond to 78 and 298 K, respectively. Observed Raman shifts (Ref. 56) are indicated by arrows.

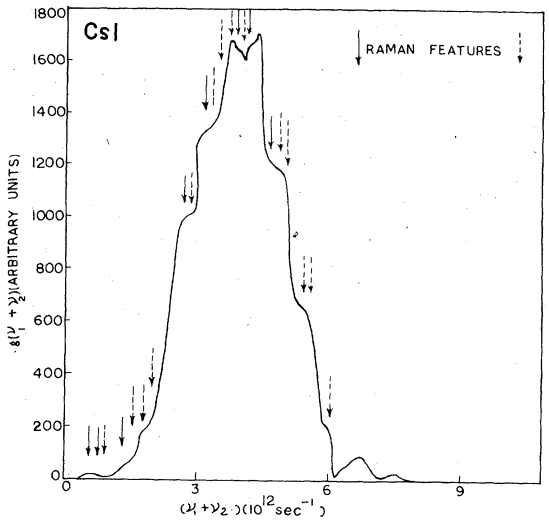

FIG. 15. Combined-density-of-states curves for CsI. Observed Raman shifts: solid arrows (Ref. 59); dashed arrows (Ref. 56).

and infrared (ir) spectra and the Debye-temperature variations. These properties are, respectively, sensitive to higher and lower sides of the frequency spectra and thus their successful predictions will provide additional reliable tests of the model besides the most dependable test provided by neutron-scattering dispersion curves.

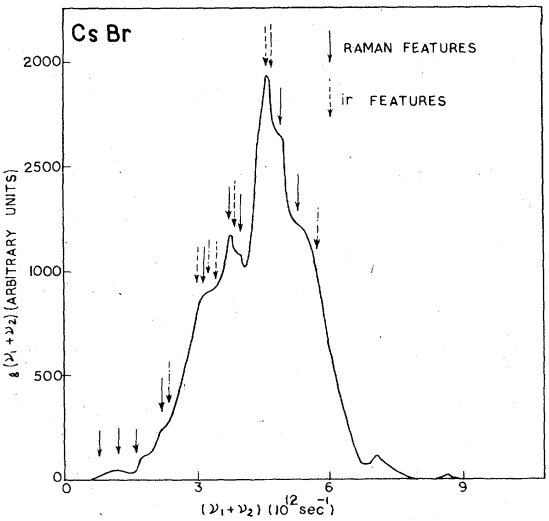

FIG. 14. Combined-density-of-states curves for CsBr. Observed Raman shifts: solid arrows (Ref. 57); dash-dot arrows (Ref. 58). Observed ir peaks: broken arrows (Ref. 43).

1. Two-phonon Raman and infrared spectra

In order to interpret the second-order infrared and Raman spectra we have employed the combined-density-of-states approach.[53] The combined-density-of-states curves have been displayed in Figs. 9–15 together with the observed peaks marked with arrows. Our theoretical peaks are generally in good agreement with the observed ones for almost all the solids studied here. In RbF, there exists a sharp peak at higher frequency and followed by three peaks of relatively weaker intensity in the low-frequency side. This feature is in accordance with that noted earlier by Hardy and Karo.[60] However, small deviations may be ascribed to the coarseness involved in the division

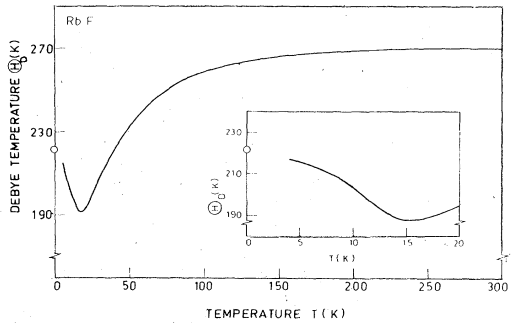

FIG. 16. Debye-temperature variations for RbF: solid line, present study; ○ represent the exactly calculated values at 0 K (Ref. 64).

TABLE V. Assignments of bands of Raman spectra.

RbF			RbCl		
		Present study			
Observed peaks (Ref. 54) (cm^{-1})	Value (cm^{-1})	Assignments	Assignments	Value (cm^{-1})	Observed peaks (Ref. 55) (cm^{-1})
89	93	$TO(L)-TA(L)$	$LO(L)-TO(L)$	32	(35)[a]
141	147	$2TA(L)$	$TO(L)-TA(L)$	44	(40)
178	176	$LO(L)-TA(L)$	$TO(X)-LA(X)$	56	55 (56)
220	221	$TO(X)+TA(X)$	$LO(X)-LA(X)$	61	58
	228	$LO(X)+TA(X)$	$LO(L)-TA(L)$	76	66 (75)
234	240	$TO(L)+TA(L)$	$TO(X)-TA(X)$	87	87 (85)
272	272	$LO(X)+LA(X)$	$LA(X)+TA(X)$	110	105 (112)
328	324	$2TO(\Gamma)$			
356	347	$2LO(X)$	$2TA(L)$	140	140
408	376	$LO(L)+LA(L)$	$TO(X)+TA(X)$	155	150 (155)
487	499	$2LO(L)$	$TO(L)+TA(L)$	184	184
572	566	$2LO(\Gamma)$	$TO(X)+LA(X)$	197	187
			$LO(X)+LA(X)$	203	198 (200)
			$TO(L)+LA(L)$	215	215
			$2TO(L)$	228	230 (230)
			$LO(L)+LA(L)$	247	235 (240)
			$2TA(\Gamma)$	250	250 (250)
			$LO(X)+TO(X)$	258	257
			$LO(L)+TO(L)$	260	260
			$2LO(X)$	264	265
			$2LO(L)$	292	(280)
			$2LO(\Gamma)$	337	(326)
			...	...	(357–432)

[a]Values enclosed within parentheses correspond to the Ref. 56.

TABLE VI. Assignments of bands of Raman spectra.

RbBr			RbI		
		Present study			
Observed peaks (Ref. 55) (cm^{-1})	Value (cm^{-1})	Assignments	Assignments	Value (cm^{-1})	Observed peaks (Ref. 55) (cm^{-1})
31	27	$LO(L)-TA(L)$	$2TA(X)$	53	51
37	39	$TO(X)-LA(X)$	$TO(X)-TA(X)$	55	55
45	40	$LO(X)-LA(X)$	$LO(X)-TA(X)$	56	60
72	63	$LO(X)-TA(X)$	$LA(X)+TA(X)$	68	69
79	83	$LA(X)+TA(X)$	...	...	75–78
108	106	$2LA(X)$	$2LA(X)$	84	80
131	124	$LO(X)+TA(X)$	...	...	85–107
150	146	$LO(X)+LA(X)$	$TO(X)+TA(X)$	108	108
154	...	...	$2TA(L)$	111	115
155	...	...	$TO(L)+TA(L)$	120	118
165	166	$LO(L)+TO(L)$	$2TO(L)$	128	127
175	185	$2TO(X)$	...	...	137–142
190	190	$LO(L)+LA(L)$	$LO(L)+TA(L)$	145	145
195	193	$2LO(L)$	$LO(L)+TO(L)$	153	150
220	264	$2LO(\Gamma)$	$2TO(\Gamma)$	162	162
			$2TO(X)$	163	163
			$2LO(X)$	165	165

TABLE VII. Assignments of Raman peaks in CsCl.

ETSM study Assignments	Value (cm^{-1})	Observed peaks (Ref. 56) value (cm^{-1})	TSM study (Ref. 14) Value (cm^{-1})	Assignments
$LA(X)-TA(X)$	42 (39)[a]	42	34	$LO(M)-TO(M)$
$LO(R)-LA(R)$	61 (59)	61	58	$LO(M)-LA(M)$
$2TA(M)$	78 (81)	81	87	$2TA(X)$
$LO(X)-TA(X)$	106 (107)	112	112	$LO(X)-TA(X)$
$LO(M)-TA(M)$	158 (158)	158	165	$LO(M)+TA(M)$
$2LA(X)$	171 (166)	170	181	$2LA(X)$
$2TO(\Gamma)$	211 (202)	212	209	$2TO(\Gamma)$
$2LO(X)$	303 (303)	310	311	$2LO(X)$
$2LO(\Gamma)$	323 (315)	353	329	$2LO(\Gamma)$

[a]Values within parentheses correspond to 298 K.

of the Brillouin zone. The agreement can be improved remarkably by employing more sophisticated programs[61,62] to generate the joint-density-of-states functions.

The fine structure of Raman spectra has been interpreted by performing the critical point analysis.[63] The assignments obtained from this analysis have been listed in Tables V–IX. Our theoretical assignments of Raman bands show much better agreement with the observed data on them than those reported elsewhere by Lal and Verma[13,14] and Haridasan and Krishnamurthy.[40]

A detailed investigation of the second-order spectra presented above is intended to provide a reliable test of ETSM which is sensitive to the higher range of phonon spectra. These studies will also be useful in correlating the neutron and optical data, deducing the individual phonon frequencies and studying the optical properties of solids to explain the considerable coupling between modes of vibrations of the ions.

2. *Debye-temperature variations*

The Debye temperatures derived from the phonon spectra have been plotted against temperatures (0 to 300 K) in Figs. 16–22. These variations have been compared with measured data for all the solids except for RbF. As expected, the agreement between theory and experiment is good for the lower range of temperatures. The theoretical values of Debye temperatures obtained by Varshini and Konti[64] have also been shown in Figs. 16–19. The results at higher temperatures

TABLE VIII. Assignments of Raman peaks in CsBr.

ETSM study Assignments	Value (cm^{-1})	Observed peaks (Ref. 57) value (cm^{-1})	TSM study (Ref. 14) Value (cm^{-1})	Assignments
$LO(X)-TO(X)$	28	25	23	$LA(X)-TO(X)$
$LO(M)-LA(M)$	35	40	42	$LA(X)-TA(X)$
$LO(M)-TA(M)$	53	54	56	$LO(X)-TA(X)$
$2TA(M)$	79	75 (79)[a]	81	$2TA(M)$
$TO(M)+TA(M)$	101	105	100	$TO(M)+TA(M)$
$TO(X)+TA(X)$	109	(107)	108	$TO(X)+TA(X)$
$LA(X)+TA(X)$	124	125	127	$2TO(X)$
$LO(M)+TA(M)$	131	134	130	$LA(X)+TA(X)$
$LO(X)+TA(X)$	137	(135)	132	$2LA(R)$
$LO(X)+TO(X)$	156	(155)	155	$2TO(\Gamma)$
$2LO(R)$	165	165	164	$LO(X)+TO(X)$
$LO(X)+LA(X)$	171	176	177	$2LO(R)$
$2LO(X)$	184	(190)	186	$LO(X)+LA(X)$

[a]Values within parentheses correspond to Ref. 58.

TABLE IX. Assignments of Raman peaks in CsI.

ETSM study Assignments	Value (cm^{-1})	Observed peaks (Ref. 56) value (cm^{-1})		TSM study (Ref. 14) Value (cm^{-1})	Assignment
$LA(X)-TO(X)$	20	20	(19)[a]	...	...
$LA(X)-TA(X)$	21	22	(22)	24	$LA(X)-TO(X)$
$LO(X)-TO(X)$	29	28		27	$LA(X)-TA(X)$
$LA(M)-TA(M)$	33	44	(44)	36	$LO(X)-TA(X)$
...	...	52		...	...
...	...	61	(61)	...	...
$2TA(X)$	82	67		81	$2TA(M)$
$2LA(M)$	89		(91)	90	$2LA(M)$
...	...	94	(94)	92	$2TO(X)$
$LA(X)+TO(X)$	105	107	(106)	...	...
$LO(X)+TA(X)$	112	...	(110)	...	...
$LO(X)+TO(X)$	113	113		113	$LO(M)+TA(M)$
$2LO(R)$	123	122		122	$LO(X)+TA(X)$
$2LA(X)$	125		(124)	125	$LO(X)+TO(X)$
$2TO(\Gamma)$	131	128		129	$2TO(\Gamma)$
$LO(X)+LA(X)$	133	135		...	...
$2LO(X)$	142		(137)	139	$2LA(X)$
$2LO(M)$	151	160	(155)	158	$2LO(X)$
$2LO(\Gamma)$	171	167		...	...
...	...	180	(181)	...	...
...	...	184		187	$2LO(\Gamma)$
...	...	200		...	...

[a]Values within parentheses correspond to Ref. 59.

have not been reproduced well not only with ETSM but also by DDM,[35] TSM,[13] and RSM.[17,26] This feature is not surprising because all these models are subject to the harmonic approximations.

In case of cesium halides, the agreement achieved from ETSM is much better than those obtained by the application of other models.[14,29,32-34] The Debye-temperature variations in the case of CsCl obtained both at 78 and 298 K and plotted in Fig. 20 show that a low-temperature curve is able to explain only the variations corresponding to lower temperature, while the curve corresponding to higher temperatures explains fairly well the variation of Debye temperature. However, the shell model used by Carabatos and Prevot[33] fails to explain the same even at low temperatures.

C. Other remarkable consequences of ETSM

It is seen from Table III that mechanical polarizabilities of cations and anions (i.e., d_1 and d_2) in

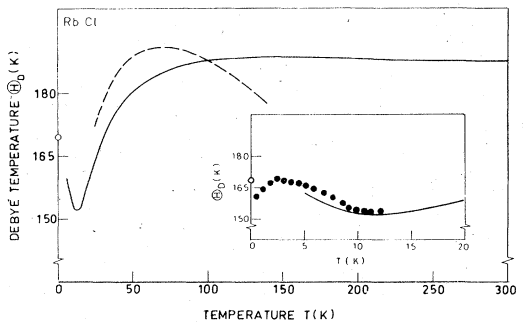

FIG. 17. Debye-temperature variations for RbCl: solid line, present study; dashed line, experimental curve (Ref. 65); ●, experimental points (Ref. 66). ○ represents the exactly calculated value at 0 K (Ref. 64).

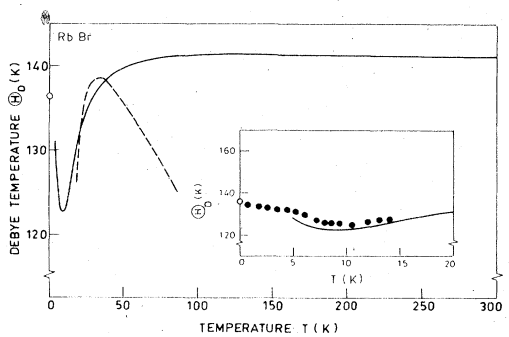

FIG. 18. Debye-temperature variations for RbBr: solid line, present study; dashed line, experimental curve (Ref. 67); ●, experimental points (Ref. 66). ○ represents the exactly calculated value at 0 K (Ref. 64).

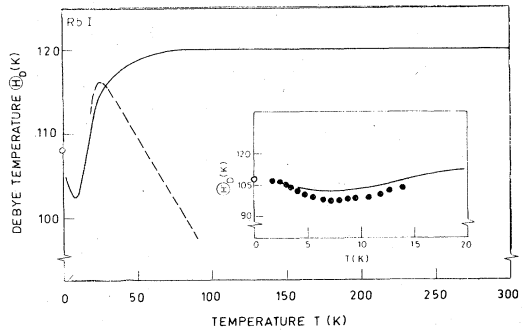

FIG. 19. Debye-temperature variation for RbI: solid line, present study; dashed line, experimental curve (Ref. 67); ●, experimental points (Ref. 66). ○ represents the exactly calculated value at 0 K (Ref. 64).

the case of RbF are almost equal. This feature is in accordance with Cochran's approach,[71] according to which the values of d_1 and d_2 are almost equal in RbF so that the value of Szigeti effective charge e^*/e $(=1+d_1-d_2)$ may not deviate from unity.

The prediction of electronic polarizabilities α_1 (α_2) of positive (negative) ions obtained from the modified Lorentz-Lorenz relation[22] have been listed in Table X and compared with various experimental and theoretical values. It is seen that all theoretical models have predicted polarizabilities generally lower than those of Tessmann *et al.*[25] This reduction may be ascribed to various kinds of operative interactions which have been ignored in the derivation of original Lorentz-Lorenz relation.[23] In the present case this reduction is due to three-body forces. The polarizabilities predicted by these models have been found to be more evenly shared by the ions than those predicted experimentally.[18,25]

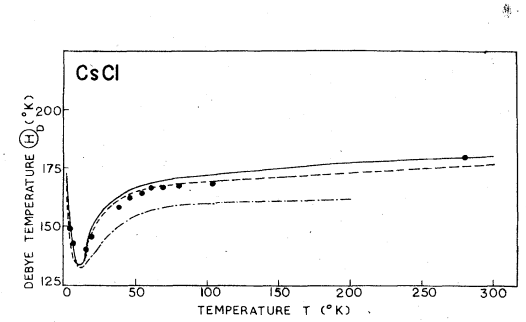

FIG. 20. Debye-temperature variations for CsCl: ETSM theoretical curves: solid lines (78 K); dashed lines (298 K); dash-dot lines (Ref. 33); ●, experimental points (Ref. 68).

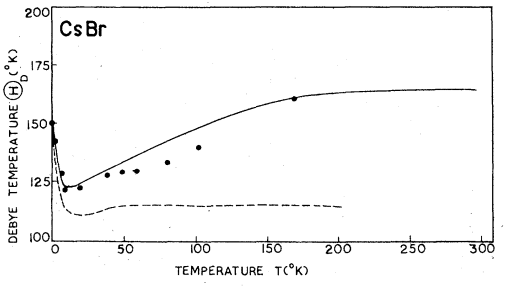

FIG. 21. Debye-temperature variations for CsBr. Theoretical curves: solid lines (ETSM); dashed lines (Ref. 33); ●, experimental points (Ref. 69).

III. GENERAL CONCLUSIONS

The overall fair agreement achieved with different experimental measurements discussed above leads to the conclusion that (i) ETSM in its framework describes both elastic and dielectric properties simultaneously, (ii) the second-neighbor short-range forces play an important role in the dynamical and dielectric descriptions, (iii) the three-body force parameters, while introducing important modifications in various macroscopic relations,[72-74] leave the Lyddane-Sachs-Teller relations[75] unchanged, and (iv) the lower temperature variatons of Debye temperatures are explained more satisfactorily than those corresponding to higher temperatures.

Despite these successes the ETSM has revealed some features which do not have much physical significance. This is evident from the table of parameters where the shell charge parameter for Cs^+ has its value 6 in CsBr and 28 in CsI, while the halide shell charge parameters have its value 3.5 in both the cases. From this physical significance viewpoint the ETSM does not seem to be qualitatively much superior to other multi-

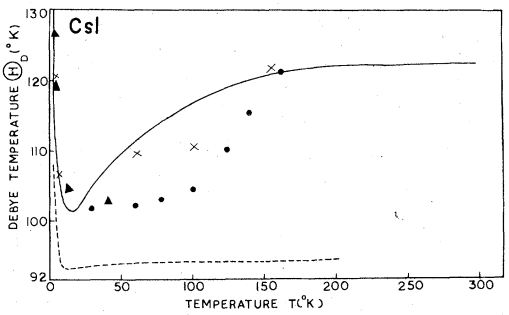

FIG. 22. Debye-temperature variations for CsI. Theoretical curves: solid line (ETSM); dashed line (Ref. 33); experimental points (●, Ref. 68), (X, Ref. 69), (▲, Ref. 70).

TABLE X. Electronic polarizabilities α_1 (α_2) (units of Å^3).

Authors	Solids RbF	RbCl	RbBr	RbI	CsCl	CsBr	CsI
Present study	1.21(0.90)	1.11(2.91)	1.66(3.49)	1.72(5.58)	2.798(2.653)	3.033(3.994)	3.131(6.191)
Tessman *et al.* (Ref. 25)	1.98(0.652)	1.98(2.97)	1.98(4.17)	1.98(6.44)	3.137(2.974)	3.137(4.130)	3.137(6.199)
Pauling (Ref. 18)	1.40(1.04)	1.40(3.66)	1.40(4.77)	1.40(7.10)	•••	•••	•••
Rolandson and Raunio (Ref. 26)	•••	•••	3.04(0.56)	2.29(5.64)	•••	•••	•••
Ahmed *et al.* (Ref. 29)	•••	•••	•••	•••	1.477(2.364)	•••	•••
Rolandson and Raunio (Ref. 32)	•••	•••	•••	•••	•••	1.19±0.66 (2.10±0.67)	•••
Büherer and Hälg (Ref. 34)	•••	•••	•••	•••	•••	•••	1.085(6.847)

parameter shell models. However, quantitatively the ETSM seems to be the best of the available multiparameter shell models for alkali halides.

To summarize, we may remark that ETSM is able to describe the elastic, dielectric, optical, and thermophysical properties of heavier alkali halides with the same success as it has done for the light weight alkali halides.[2,76,77] This gives us confidence that ETSM is a reasonably realistic and appropriate model for the description of the lattice dynamics of alkali halides.

ACKNOWLEDGMENTS

The authors are grateful to Professor B. S. Mathur, Vice Chancellor, Meerut University and to Dr. P. C. Gupta, Principal of N. R. E. C. College for their keen interest and encouragements. They are also thankful to the University Grants Commission, Delhi for the research grant and to the Director, computer center, Aligarh Muslim University for the permission to use their IBM 1130 computer.

[1]R. K. Singh and H. N. Gupta, Proc. R. Soc. Lond. A 349, 289 (1976).
[2]R. K. Singh and K. Chandra, Phys. Rev. B 14, 2625 (1976).
[3]R. K. Singh and M. K. Agrawal, Solid State Commun. 17, 991 (1975).
[4]R. K. Singh and H. N. Gupta, Solid State Commun. 16, 197 (1975).
[5]P. O. Löwdin, Ark. Mat. Astron. Fys. 35A, 30 (1947).
[6]S. Q. Lundqvist, Ark. Fys. 9, 435 (1955).
[7]M. P. Verma and R. K. Singh, Phys. Status Solidi 33, 769 (1969).
[8]A. D. B. Woods, W. Cochran, and B. N. Brockhouse, Phys. Rev. 119, 980 (1960).
[9]A. M. Karo and J. R. Hardy, Phys. Rev. 129, 2024 (1963).
[10]R. K. Singh and M. P. Verma, Phys. Rev. B 2, 4288 (1970).
[11]M. P. Verma and R. K. Singh, J. Phys. C 4, 2749 (1971).
[12]M. P. Verma and H. H. Lal, Phys. Status Solidi 38, K19 (1970).
[13]H. H. Lal and M. P. Verma, J. Phys. C 5, 543 (1972).
[14]H. H. Lal and M. P. Verma, J. Phys. C 5, 1038 (1972).
[15]J. R. Hardy, Philos. Mag. 4, 1278 (1959); 5, 859 (1960); 6, 27 (1961); 7, 315 (1962).
[16]J. R. Hardy, in *Dynamical Properties of Solids*, Vol. I, edited by G. K. Horton and A. A. Maradudin (Elsevier, Amsterdam, 1974), p. 157.
[17]G. Raunio and S. Rolandson, J. Phys. C 3, 1013 (1970).
[18]L. Pauling, Proc. R. Soc. Lond. A 114, 181 (1927).
[19]J. J. O'Dwyer and H. H. Nickle, Phys. Rev. B 2, 5063 (1970).
[20]R. P. Lowndes and D. H. Martin, Proc. R. Soc. Lond. A 308, 473 (1969).
[21]Extrapolated to 80 °K from the room-temperature value [see C. Kittel, Introduction to Solid State Physics (Wiley, New York, 1956), p. 80.
[22]B. J. Marshall, D. O. Pederson, and S. S. Dorris, J. Phys. Chem. Solids 28, 1061 (1967).
[23]M. Born and K. Huang, *Dynamical Theory of Crystal Lattice* (Clarendon, Oxford, 1954), p. 54.
[24]J. T. Lewis, A. Lehoczky, and C. V. Briscoe, Phys. Rev. 161, 877 (1967).
[25]J. R. Tessmann, A. H. Kahn, and W. Schockley, Phys. Rev. 92, 890 (1953).
[26]S. Rolandson and G. Raunio, J. Phys. C 4, 958 (1971).
[27]G. Raunio and S. Rolandson, Phys. Status Solidi 40, 749 (1970).
[28]O. D. Slagle and H. A. Mackinstry, J. Appl. Phys. 38, 451 (1967).
[29]A. A. Z. Ahmed, H. S. Smith, N. Wakabayashi, and M. K. Wilkinson, Phys. Rev. B 6, 3956 (1972).
[30]S. Mahler and U. Schröder, *Proceedings of the International Conference on Phonons, Rennes, France*, edited by M. A. Nusimovici (Flamarion, Paris, 1971), p. 89.
[31]K. Reinitz, Phys. Rev. 123, 615 (1961).
[32]S. Rolandson and G. Raunio, Phys. Rev. B 4, 4617 (1971).
[33]C. Carabotos and B. Prevot, Can. J. Phys. 50, 122 (1972).
[34]W. Büherer and W. Hälg, Phys. Status Solidi 46, 679 (1971).
[35]A. M. Karo (private communication).
[36]A. M. Karo, J. Chem. Phys. 33, 7 (1960).

[37]Sneh and B. Dayal, Phys. Status Solidi B67, 125 (1975).
[38]R. N. Pandey and B. Dayal, Solid State Commun. 11, 185 (1972).
[39]W. Kress, Phys. Status Solidi B 62, 403 (1974).
[40]T. M. Haridasan and N. Krishnamurthy, Ind. J. Pure Appl. Phys. 6, 407 (1968).
[41]U. Schröder, Solid State Commun. 4, 347 (1966).
[42]S. Rolandson, Phys. Status Solidi B 52, 643 (1972).
[43]N. Krishnamurthy and T. M. Haridasan, Ind. J. Pure Appl. Phys. 1, 337 (1963).
[44]S. Ganesan and R. Srinivasan, Proc. R. Soc. Lond. A 271, 154 (1963).
[45]B. Sharan and L. M. Tiwari, Phys. Status Solidi 7, 39 (1964); 8, 265 (1965).
[46]J. D. Dheer and B. Sharan, Phys. Status Solidi 9, 701 (1965).
[47]J. F. Vetelino, S. S. Mitra, and K. V. Namjoshi, Phys. Rev. B 2, 2167 (1967).
[48]G. P. Srivastava and B. Dayal, Can. J. Phys. 45, 3339 (1967).
[49]T. M. Haridasan, N. Krishnamurthy, and J. Govindarajan, J. Ind. Inst. Sci. 50, 200 (1968).
[50]A. M. Karo and J. R. Hardy, J. Chem. Phys. 48, 3173 (1968).
[51]G. Mahler and P. Engelhardt, Phys. Status Solidi B 45, 543 (1971).
[52]J. Daubert, Phys. Lett. A 32, 437 (1970).
[53]C. Smart, G. H. Wilkinson, A. M. Karo, and J. R. Hardy, Z. Phys. 99, 387 (1963).
[54]R. R. Hayes and K. H. Rieder, Phys. Rev. B 8, 5972 (1973).
[55]J. E. Potts and Charles T. Walker, Phys. Rev. B 8, 2756 (1973).
[56]A. I. Stekhnov and A. P. Korol'Kov, Sov. Phys.-Solid State 8, 734 (1966).
[57]A. I. Stekhnov and A. P. Korol'Kov, Sov. Phys.-Solid State 4, 231 (1963).
[58]P. S. Narayanan, Proc. Ind. Acad. Sci. A 42, 304 (1955).
[59]N. Krishnamurthy and R. S. Krishnan, Ind. J. Pure Appl. Phys. 1, 239 (1963).
[60]J. R. Hardy and A. M. Karo, *Proceedings of the International Conference on Lattice Dynamics, Copenhagen, 1965*, edited by R. F. Wallis (Pergamon, London, 1965).
[61]G. Dolling and R. A. Cowley, Proc. Phys. Soc. Lond. 88, 463 (1966).
[62]G. Gilat and L. J. Raubenheimer, Phys. Rev. 144, 390 (1966).
[63]E. Burstein, F. A. Johnson, and R. Loudon, Phys. Rev. 139, 1239 (1965).
[64]Y. P. Varshini and A. Konti, J. Phys. C 5, 2561 (1962).
[65]A. J. Kirkham and B. Yates, Cryogenics 8, 381 (1968).
[66]R. J. Rollefson and P. P. Peressini, J. Appl. Phys. 43, 727 (1972).
[67]K. Clausius, J. Goldmann, and A. Perlick, Z. Naturf. 4A, 424 (1949).
[68]A. H. Taylor, T. E. Gardner, and D. F. Smith, U. S. Bur. Mines Rept. Invest. No. 6157 (1963) (unpublished).
[69]M. Sorai, J. Phys. Soc. Jpn. 25, 421 (1968).
[70]B. J. Marshall and J. R. Kunkel, J. Appl. Phys. 40, 519 (1969).
[71]W. Cochran, Philos. Mag. 4, 1082 (1962).
[72]Lorentz-Lorenz and Clausius-Mosotti relations, see Ref. 23.
[73]A. R. Ruffa, Phys. Rev. 130, 1412 (1963); 133, 1408 (1964).
[74]B. Szigeti, Proc. R. Soc. Lond. A 252, 217 (1959); 258, 337 (1960).
[75]R. H. Lyddane, R. Sachs, and F. Teller, Phys. Rev. 59, 673 (1941).
[76]R. K. Singh and K. Chandra (private communication).
[77]R. K. Singh, Rep. Prog. Phys. (to be published).